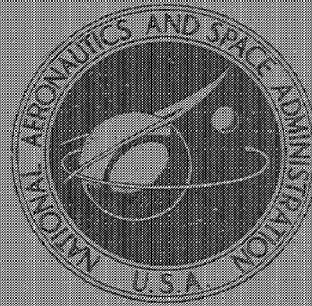


171-28121

NASA TECHNICAL
MEMORANDUM



NASA TM X-2260

NASA TM X-2260

CASE FILE
COPY

LUNAR GRAVITATIONAL FIELD:
A THIRTEENTH DEGREE AND ORDER
SPHERICAL HARMONIC ESTIMATE

by W. T. Blackshear, E. F. Daniels, and S. G. Anderson

Langley Research Center

Hampton, Va. 23365

1. Report No. NASA TM X-2260	2. Government Accession No.	3. Recipient's Catalog No.	
4. Title and Subtitle LUNAR GRAVITATIONAL FIELD: A THIRTEENTH DEGREE AND ORDER SPHERICAL HARMONIC ESTIMATE		5. Report Date June 1971	
		6. Performing Organization Code	
7. Author(s) W. Thomas Blackshear, Edward F. Daniels, and S. G. Anderson		8. Performing Organization Report No. L-7401	
		10. Work Unit No. 130-06-07-05	
9. Performing Organization Name and Address NASA Langley Research Center Hampton, Va. 23365		11. Contract or Grant No.	
		13. Type of Report and Period Covered Technical Memorandum	
12. Sponsoring Agency Name and Address National Aeronautics and Space Administration Washington, D.C. 20546		14. Sponsoring Agency Code	
		15. Supplementary Notes	
16. Abstract Lunar Orbiter tracking data have been analyzed to yield a thirteenth degree and order spherical harmonic approximation to the lunar gravitational potential function. The results of the analysis indicate an essentially homogeneous moon and demonstrate a correlation between lunar surface features and gravitational anomalies. In addition, a correlation exists between the type of data coverage and the general character of acceleration anomalies calculated from the potential approximation.			
17. Key Words (Suggested by Author(s)) Lunar gravitational field Gravitational field anomalies		18. Distribution Statement Unclassified - Unlimited	
19. Security Classif. (of this report) Unclassified	20. Security Classif. (of this page) Unclassified	21. No. of Pages 18	22. Price* \$3.00

LUNAR GRAVITATIONAL FIELD: A THIRTEENTH DEGREE
AND ORDER SPHERICAL HARMONIC ESTIMATE

By W. Thomas Blackshear, Edward F. Daniels,
and S. G. Anderson
Langley Research Center

SUMMARY

Lunar Orbiter tracking data have been analyzed to yield a thirteenth degree and order spherical harmonic approximation to the lunar gravitational potential function. The results of the analysis indicate an essentially homogeneous moon and demonstrate a correlation between lunar surface features and gravitational anomalies. In addition, a correlation exists between the type of data coverage and the general character of acceleration anomalies calculated from the potential approximation.

INTRODUCTION

Since the first of the Lunar Orbiter missions in August 1966, radar tracking data from the Orbiter spacecraft have been intensively analyzed to obtain a better definition of the gravitational field of the moon. (See refs. 1 to 6.) These investigations have assumed a spherical harmonic expansion of the lunar gravitational potential function similar to the one used in this analysis:

$$U = \frac{GM}{r} \left[C_{0,0} + \sum_{n=2}^{\infty} \sum_{m=0}^n \left(\frac{a}{r} \right)^n P_{n,m} \sin \phi (C_{n,m} \cos m\lambda + S_{n,m} \sin m\lambda) \right]$$

Each of these studies has been an attempt to define a sufficient number of the coefficients $C_{n,m}$ and $S_{n,m}$ to yield a "good" approximation of the lunar gravitational field. The results of these studies have demonstrated that the mathematical representation of the observed data is to some extent either erroneous (because of unmodeled sources of bias) or incomplete (because of truncation of the potential series). These two possibilities are evidenced by systematic residuals in the fit to the tracking data. The present analysis has been conducted under the philosophy that the principal inadequacy in the mathematical model lies in the representation of localized lunar gravitational anomalies. Hence, the finite-term approximation to the lunar potential function has been extended to the thirteenth degree and order in an attempt to provide better resolution of

these anomalies. Some success has been achieved in the curve-fitting aspects of this approach. However, a systematic residual pattern is still evident and points out a remaining model incompleteness; possibly, the dominant contribution is from localized gravitational anomalies.

SYMBOLS

A	principal moment of inertia about selenographic X-axis
a	radius of moon, 1738.09 km
B	principal moment of inertia about selenographic Y-axis
C	principal moment of inertia about selenographic Z-axis
$C_{n,m}, S_{n,m}$	coefficients of lunar gravitational potential harmonics
GM	product of gravitational constant G and lunar mass M, $4902.58 \text{ km}^3/\text{sec}^2$
M	lunar mass
$P_{n,m}$	associated Legendre polynomials of degree n and order m
r	selenographic radius, km
U	gravitational potential function, km^2/sec^2
X,Y,Z	selenographic axes
λ	selenographic longitude, deg
ϕ	selenographic latitude, deg

DISCUSSION AND RESULTS

Method of Analysis and Data Coverage

Table I presents approximate orbital characteristics for those phases of the Lunar Orbiter missions from which data have been analyzed in a weighted-least-squares, differential-correction process. Fundamental to this process is the numerical integration

of the spacecraft trajectory (Cowell formulation) and the associated variational equations utilizing a twelfth-order predictor-correction technique with 13-digit precision. Initial values specified for the spacecraft state and the lunar gravitational coefficients are then differentially corrected and the procedure is iterated to achieve a least-squares fit to observed data. These observations consist of counting, over 1-minute intervals, the number of cycles in the Doppler frequency shift in a radio signal sent from an earth station to the spacecraft, where it is retransmitted to an earth receiving station.

The lower part of table I gives a breakdown of the data into the number of data arcs (data representing a continuous spacecraft trajectory), number of data points, and total length of coverage per orbiter provided by these arcs.

The total data currently analyzed amounts to 20 148 coherent two-way Doppler observations representing approximately 80 days of tracking. This direct observational coverage is illustrated in figures 1 and 2 for the total data and for data taken when the spacecraft was below 200 km in altitude, respectively. Because of the line-of-sight characteristic of the radar tracking system, direct observation of the spacecraft is interrupted as it moves behind the moon. The selenographic longitude of the spacecraft at this interruption depends upon the altitude of the spacecraft above the lunar surface. It follows that direct observations relating to the lunar far-side environment must be at relatively high altitude, as compared with near-side observations. As a result of radial attenuation of gravitational effects, these data are less sensitive to localized gravitational anomalies than the near-side data which represent a much wider range of altitudes. Comparison of figures 1(b) and 2(b) shows the impact of this altitude constraint on the data coverage. Comparison of figures 1(a) and 1(b) with figures 2(a) and 2(b) gives an implication of the relative sensitivity to localized gravitational anomalies of near-side data compared with far-side data. This high-altitude constraint also applies to a lesser degree to the polar regions because of mission design which required periapse photography of near-equatorial sites.

An additional point with regard to figure 1 is that although areas are shown in which no direct observations were taken, these regions are indirectly represented in the data. This is true in the sense that the path of the spacecraft over these areas is included in at least one of the continuous arcs used in the analysis. Thus, the net effect of the gravitational forces in these regions is reflected in the spacecraft trajectory and hence in the data. However, the absence of direct data and/or low-altitude data remains as an important limitation in view of the current incompleteness of the mathematical model. Consequences of this limitation are pointed out later in relation to gravitational contour maps.

Estimates of the Lunar Gravitational Coefficients

Estimates of the gravitational harmonic coefficients through degree and order thirteen are given in table II. The estimate given for $C_{0,0}$ implies a value of $4902.84 \text{ km}^3/\text{sec}^2$ for GM. In view of the preceding discussions relating to model incompleteness and data coverage, these numbers should be considered as interim estimates, subject to later refinement. Caution should be exercised in interpreting the numbers in table II, since their validity as gravitational field estimates requires use of the complete set of coefficients. For example, based on a sequence of unpublished gravitational field estimates of different degrees (generated by the first author in analysis of varying combinations of data), the field estimates are relatively stable, whereas the dispersion in individual coefficient estimates indicates that they are accurate only to within an order of magnitude. Exceptions to this rule are GM and the coefficients C_{20} , C_{22} , and C_{31} . Table III presents values of these parameters. The parameter uncertainties listed with the current estimates in column 5 of table III are based on the dispersion of this sequence of values about the current estimates.

Implications of the Gravitational Field Estimates

Contour maps of the radial component of acceleration corresponding to the current estimate of the lunar gravitational field are given in figure 3. These contours are in milligals ($10^{-3} \text{ cm}/\text{sec}^2$) and represent the deviation in the radial acceleration from that of a spherically symmetric field, for which $GM = 4902.84 \text{ km}^3/\text{sec}^2$, at an altitude of 100 km. The three large Northern Hemisphere positive anomalies occurring below a latitude of 40° in figure 3(a) correspond closely to the lunar maria Imbrium, Serenitatis, and Crisium. (Refer to the lunar map given in fig. 4.) These three anomalies are in substantial agreement with results given in references 7 and 8. Comparison of figure 3(a) with figure 1(a) shows relatively dense direct data coverage of these areas with the exception of the northernmost portion of the Serenitatis anomaly. This fact, coupled with the relative stability of these anomalies throughout the analysis, leads the authors to the conclusion that these contour anomalies are reasonable representations of true lunar gravitational anomalies. In contrast to these areas, consider the large positive anomaly at longitude, -60° ; latitude, -35° . Inspection of figure 1(a) shows this anomaly to lie in a region devoid of direct observational data. This result may be more than an interesting coincidence because if the general "roughness" of figure 3(a) is compared with the general data coverage, implied by the combination of figures 1(a) and 2(a), a correlation between contour "roughness" and the relative sensitivity of the data to localized gravitational anomalies is apparent. If this type of comparison is extended to the lunar far side, the correlation becomes even more apparent from the alternating high-low nature of the contours and their increase in amplitude up to approximately 1000 milligals ($1 \text{ cm}/\text{sec}^2$) in the region of 180° longitude. It seems likely that the general "roughness" of the

gravitational field estimate, although induced by localized gravitational anomalies, is more representative of the currently incomplete mathematical model of the data and the curve-fitting philosophy of the least-squares method. It is believed that these factors lead to a biased estimate in the areas of least sensitive data coverage in order to achieve a more valid estimate in the areas of most sensitive coverage. For this reason, no attempt has been made to correlate the current estimate of gravitational anomalies in the polar and far-side regions with lunar surface features.

In spite of the low confidence level assigned to most of the individual gravitational coefficients, the stability of certain low-degree coefficients permits some reasonable inferences to be drawn. In particular, the second-degree coefficients can be related to the lunar moments of inertia (ref. 9) under the assumption that $(C - A)/B = 0.000629$. Table IV lists the associated selenographic inertia tensor and the principal moments of inertia based on the values in table II. Uncertainties given for the principal moments are estimated from the dispersion resulting from use of the sets of second-degree coefficients associated with the gravitational field estimates of table III. These estimates indicate that the lunar principal axes differ from the selenographic axes by no more than 5.5° and imply an essentially homogenous moon. ($C/Ma^2 = 0.4$ for a homogeneous sphere.)

The mare-associated gravitational anomalies discussed earlier present a contrast to the basic homogeneity implied by the moment-of-inertia estimates. To achieve a rough estimate of a possible density distribution causing these anomalies, point-source approximations were used for the Imbrium and Serenitatis anomalies. The gravitational field of these point sources was expanded in spherical harmonics to the same degree and order as the current estimate of the lunar gravitational field. By the method of least squares, this expansion was then fitted to the lunar gravitational-field estimate over regions in space varying from 50 to 150 kilometers in altitude and 10° in selenocentric angle from the "axis" of the anomaly. The resulting solutions for the masses and locations of the point sources are given in table V and indicate, as one explanation, large mass concentrations at depths of approximately 200 and 300 kilometers. Figure 5 illustrates the degree of agreement between the point-source solution and the current spherical harmonic estimate of the Serenitatis anomaly. Although the gravitational-field analysis is not sufficiently stable to justify an exhaustive interpretative analysis, the preceding exercise illustrates the type of investigations that can be conducted with a more refined gravitational-field estimate and more elaborate source models.

CONCLUDING REMARKS

The preceding results represent the current status of a continuing analysis. Problem areas associated with mathematical modeling, observational data coverage, and the effect of these areas on the validity of the analysis have been alluded to. Specifically, a

strong correlation has been shown to exist between the type of data coverage and the general "roughness" of the current gravitational-field estimate. This correlation, in connection with the instability of the lunar far-side gravitational contours, indicates that current estimates of localized gravitational anomalies on the lunar far side are not physically valid. However, the stability of the estimates of the near-side gravitational contours permits a reliable association of gravitational anomalies with certain lunar maria. Also, the stability of the low degree and order harmonic coefficients yields a reliable implication that the moments of inertia of the moon are very nearly those of a spherical, homogeneous body.

Langley Research Center,
National Aeronautics and Space Administration,
Hampton, Va. April 30, 1971.

REFERENCES

1. Michael, William H., Jr.; Tolson, Robert H.; and Gapcynski, John P.: Preliminary Results on the Gravitational Field of the Moon From Analysis of Lunar Orbiter Tracking Data. *Trans. Amer. Geophys. Union*, vol. 48, no. 1, Mar. 1967, p. 55.
2. Tolson, Robert H.; and Gapcynski, John P.: An Analysis of the Lunar Gravitational Field as Obtained From Lunar Orbiter Tracking Data. Paper presented at IQSY/COSPAR Assemblies (London, England), July 17-28, 1967.
3. Michael, William H., Jr.: Physical Properties of the Moon as Determined From Lunar Orbiter Data. Paper presented at Fourteenth General Assembly of the International Union of Geodesy and Geophysics Meeting (Lucerne, Switzerland), Sept.-Oct. 1967.
4. Lorell, J.; and Sjogren, W. L.: Lunar Gravity: Preliminary Estimates From Lunar Orbiter. *Science*, vol. 159, no. 3815, Feb. 9, 1968, pp. 625-627.
5. Gapcynski, John P.; Blackshear, W. Thomas; and Compton, Harold R.: Lunar Gravitational Field as Determined From Lunar Orbiter Tracking Data. *AIAA J.*, vol. 7, no. 10, Oct. 1969, pp. 1905-1908.
6. Blackshear, W. Thomas: Progress on Lunar Gravitational Potential Determination by Analysis of Lunar Orbiter Tracking Data. Paper presented at 50th Amer. Geophysical Union Annual Meeting (Washington, D.C.), Apr. 1969.
7. Muller, P. M.; and Sjogren, W. L.: Mascons: Lunar Mass Concentrations. *Science*, vol. 161, no. 3842, Aug. 16, 1968, pp. 680-684.
8. Gottlieb, P.: Lunar Gravimetric Maps. The Deep Space Network for the Period September 1 to October 31, 1969. *Space Programs Sum. No. 37-60, Vol. II* (Contract No. NAS 7-100), Jet Propulsion Lab., California Inst. Technol., Nov. 30, 1969, pp. 106-109.
9. Michael, W. H., Jr.; Blackshear, W. Th.; and Gapcynski, J. P.: Results on the Mass and the Gravitational Field of the Moon as Determined From Dynamics of Lunar Satellites. *Dynamics of Satellites*, Bruno Morando, ed., Springer-Verlag, 1970, pp. 42-56.

TABLE I.- ORBITAL GEOMETRY AND TRACKING DATA

	Lunar Orbiter					
	I	II	IIIa	IIIb	IV	V
Semimajor axis, km	2670	2702	2688	1968	3751	2832
Eccentricity	0.327	0.341	0.332	0.062	0.516	0.317
Inclination,* deg	12	18	21	21	84	85
Period, min	206	210	208	130	344	225
Data arcs	2	3	3	5	2	8
Total length of arcs, days	9.7	8.5	15.9	17.1	8.6	19.9
Observations	2076	2662	2502	3322	3739	5847

*Inclination to lunar equator.

TABLE II.- COEFFICIENTS OF THE THIRTEENTH DEGREE AND ORDER SOLUTION
FOR LUNAR GRAVITATIONAL FIELD

n	m	C _{n,m}	S _{n,m}
0	0	1.00005388274	-----
2	0	-2.0378761820 x 10 ⁻⁴	0
1	1	1.1051542512 x 10 ⁻⁵	1.3006148287 x 10 ⁻⁵
2	2	2.4845211490 x 10 ⁻⁵	-1.0442661244 x 10 ⁻⁸
3	0	2.8439912986 x 10 ⁻⁵	0
1	1	2.4152698939 x 10 ⁻⁵	2.0805931299 x 10 ⁻⁵
2	2	7.6322652451 x 10 ⁻⁶	2.2710804784 x 10 ⁻⁶
3	3	1.4111967268 x 10 ⁻⁶	-3.1126414977 x 10 ⁻⁷
4	0	3.4688330254 x 10 ⁻⁵	0
1	1	-1.9891933273 x 10 ⁻⁵	-8.5100449545 x 10 ⁻⁶
2	2	-2.5443614074 x 10 ⁻⁶	-4.1656170604 x 10 ⁻⁶
3	3	-5.6321036284 x 10 ⁻⁷	-2.7682641529 x 10 ⁻⁷
4	4	-5.3981736976 x 10 ⁻⁸	1.1411256460 x 10 ⁻⁷
5	0	-2.6623483022 x 10 ⁻⁵	0
1	1	-7.4939720619 x 10 ⁻⁶	-9.2535826576 x 10 ⁻⁶
2	2	3.4603507569 x 10 ⁻⁷	3.8762399793 x 10 ⁻⁷
3	3	4.0040015934 x 10 ⁻⁷	8.8773988822 x 10 ⁻⁷
4	4	9.3924925003 x 10 ⁻⁸	-1.4794482739 x 10 ⁻⁷
5	5	1.8771823966 x 10 ⁻⁸	-2.1001366939 x 10 ⁻⁸
6	0	4.9673195626 x 10 ⁻⁵	0
1	1	-1.8543318257 x 10 ⁻⁵	-9.5673010658 x 10 ⁻⁶
2	2	-5.5091031933 x 10 ⁻⁷	1.8138036159 x 10 ⁻⁷
3	3	1.1678358571 x 10 ⁻⁷	-1.1841174024 x 10 ⁻⁷
4	4	-3.3956313198 x 10 ⁻⁸	-9.7021389127 x 10 ⁻⁸
5	5	-9.6847691920 x 10 ⁻⁹	8.1237744599 x 10 ⁻⁹
6	6	-4.0790023093 x 10 ⁻⁹	2.9739566973 x 10 ⁻⁹
7	0	-7.2781850970 x 10 ⁻⁵	0
1	1	4.1810263527 x 10 ⁻⁶	-2.8408094790 x 10 ⁻⁵
2	2	-8.3378247684 x 10 ⁻⁷	-7.4166186129 x 10 ⁻⁷
3	3	-1.2737535124 x 10 ⁻⁷	-1.7509754956 x 10 ⁻⁷
4	4	-4.1682647653 x 10 ⁻⁸	-2.5407115475 x 10 ⁻⁹
5	5	1.8658206027 x 10 ⁻⁹	1.0910340047 x 10 ⁻⁸
6	6	4.6261404574 x 10 ⁻¹⁰	-7.1046094393 x 10 ⁻¹⁰
7	7	3.4334519153 x 10 ⁻¹⁰	-1.2401781124 x 10 ⁻¹⁰
8	0	-1.7411742627 x 10 ⁻⁵	0
1	1	1.3701858067 x 10 ⁻⁵	3.6716642133 x 10 ⁻⁶
2	2	4.0795796661 x 10 ⁻⁷	9.1385019071 x 10 ⁻⁷
3	3	9.3910161964 x 10 ⁻⁹	-1.9359154697 x 10 ⁻⁷
4	4	-6.4523074373 x 10 ⁻⁹	2.5059489581 x 10 ⁻⁸
5	5	4.5024517927 x 10 ⁻⁹	-9.1723952804 x 10 ⁻¹⁰
6	6	3.6434678341 x 10 ⁻¹⁰	-1.0430917747 x 10 ⁻⁹
7	7	-1.4858612477 x 10 ⁻¹¹	2.1525564980 x 10 ⁻¹¹
8	8	-3.6012675699 x 10 ⁻¹¹	1.1935027479 x 10 ⁻¹¹
9	0	-6.5011326253 x 10 ⁻⁵	0
1	1	5.3770904532 x 10 ⁻⁷	-5.2273480368 x 10 ⁻⁶
2	2	-4.4206541496 x 10 ⁻⁷	-3.1727246486 x 10 ⁻⁷
3	3	-1.2910912315 x 10 ⁻⁷	-5.4900413900 x 10 ⁻⁸
4	4	-8.3591988861 x 10 ⁻⁹	2.1240873880 x 10 ⁻⁸
5	5	8.7259392768 x 10 ⁻¹⁰	-2.5124288158 x 10 ⁻⁹
6	6	-5.1505398116 x 10 ⁻¹⁰	1.2516041989 x 10 ⁻¹⁰
9	7	-8.0690242529 x 10 ⁻¹¹	8.0754026764 x 10 ⁻¹¹
8	8	-1.2649479578 x 10 ⁻¹²	2.6681227345 x 10 ⁻¹¹
9	9	1.7805101055 x 10 ⁻¹²	-5.4376209997 x 10 ⁻¹³
10	0	-1.9534030711 x 10 ⁻⁵	0
1	1	3.5640472538 x 10 ⁻⁵	4.451233094077 x 10 ⁻⁷
2	2	4.9196310871 x 10 ⁻⁹	5.7169685637 x 10 ⁻⁷
3	3	-2.2358784038 x 10 ⁻⁹	-3.6437585575 x 10 ⁻⁸
4	4	3.9141653049 x 10 ⁻⁹	1.1269567323 x 10 ⁻⁸
5	5	3.8087666364 x 10 ⁻¹⁰	-2.1308938653 x 10 ⁻⁹
6	6	-4.6255135189 x 10 ⁻¹¹	1.5652458548 x 10 ⁻¹⁰
7	7	2.7614962503 x 10 ⁻¹¹	-1.5540376682 x 10 ⁻¹¹
8	8	5.4896743830 x 10 ⁻¹²	-4.0505042040 x 10 ⁻¹²
9	9	9.2407535252 x 10 ⁻¹⁴	-3.6136326596 x 10 ⁻¹³
10	10	-7.5223488683 x 10 ⁻¹⁴	3.3135927064 x 10 ⁻¹⁴
11	0	5.1037452530 x 10 ⁻⁵	0
1	1	-7.7291781814 x 10 ⁻⁶	2.8479446434 x 10 ⁻⁵
2	2	-3.2273658086 x 10 ⁻⁷	7.2497774428 x 10 ⁻⁷
3	3	2.3360853505 x 10 ⁻⁸	5.5966682329 x 10 ⁻⁸
4	4	1.0287849331 x 10 ⁻⁹	1.3205804852 x 10 ⁻⁸
5	5	-3.1877004821 x 10 ⁻¹⁰	-8.8603014695 x 10 ⁻¹⁰
6	6	6.2535668259 x 10 ⁻¹¹	1.2557575513 x 10 ⁻¹⁰
7	7	-1.3948668302 x 10 ⁻¹²	-1.6191981587 x 10 ⁻¹¹
8	8	-9.6800165098 x 10 ⁻¹³	2.8512390282 x 10 ⁻¹³
9	9	-2.8524797963 x 10 ⁻¹³	2.5679558039 x 10 ⁻¹³
10	10	-1.4876779292 x 10 ⁻¹⁴	2.0466569257 x 10 ⁻¹⁴
11	11	7.2963987090 x 10 ⁻¹⁶	-1.1859856626 x 10 ⁻¹⁵
12	0	9.7617164640 x 10 ⁻⁶	0
1	1	1.2778274406 x 10 ⁻⁵	1.4438415728 x 10 ⁻⁶
2	2	-1.5405505424 x 10 ⁻⁷	5.3551638732 x 10 ⁻⁷
3	3	5.4002051640 x 10 ⁻⁹	8.7868585746 x 10 ⁻⁹
4	4	4.0078293255 x 10 ⁻⁹	1.2737288951 x 10 ⁻⁹
5	5	9.5030429269 x 10 ⁻¹¹	-4.8376477908 x 10 ⁻¹⁰
6	6	1.7093579633 x 10 ⁻¹¹	6.0134093338 x 10 ⁻¹²
7	7	-7.2263198820 x 10 ⁻¹³	-5.5677059494 x 10 ⁻¹²
8	8	1.2421199266 x 10 ⁻¹³	9.7510387449 x 10 ⁻¹³
9	9	-3.7285776082 x 10 ⁻¹⁴	-2.4368928834 x 10 ⁻¹⁴
10	10	9.9312843321 x 10 ⁻¹⁵	-1.0618795919 x 10 ⁻¹⁴
11	11	5.2033681565 x 10 ⁻¹⁶	-4.2870250967 x 10 ⁻¹⁶
12	12	-2.3855459682 x 10 ⁻¹⁸	4.5543340194 x 10 ⁻¹⁸
13	0	7.5782274244 x 10 ⁻⁶	0
1	1	-5.7637379713 x 10 ⁻⁶	2.3610613996 x 10 ⁻⁵
2	2	-1.5991666946 x 10 ⁻⁷	3.4297075982 x 10 ⁻⁷
3	3	2.7190638195 x 10 ⁻⁸	9.6757608497 x 10 ⁻⁹
4	4	7.6732684554 x 10 ⁻¹⁰	3.0028913747 x 10 ⁻⁹
5	5	-2.1117612255 x 10 ⁻¹⁰	-1.1279989530 x 10 ⁻¹⁰
6	6	1.8106651096 x 10 ⁻¹¹	1.9737118563 x 10 ⁻¹¹
7	7	-1.6221201052 x 10 ⁻¹²	-1.1582995210 x 10 ⁻¹²
8	8	-8.7167027819 x 10 ⁻¹⁴	8.6768075576 x 10 ⁻¹⁴
9	9	1.0705140705 x 10 ⁻¹⁴	-2.7869365761 x 10 ⁻¹⁴
10	10	-7.5223488683 x 10 ⁻¹⁴	3.3135927064 x 10 ⁻¹⁴
11	11	-2.8387572286 x 10 ⁻¹⁶	2.0316367811 x 10 ⁻¹⁶
12	12	-9.0639928622 x 10 ⁻¹⁸	-1.2565366439 x 10 ⁻¹⁷
13	13	1.1380844737 x 10 ⁻¹⁸	-2.6006569878 x 10 ⁻¹⁹

TABLE III.- ESTIMATES OF LUNAR GRAVITATIONAL PARAMETERS

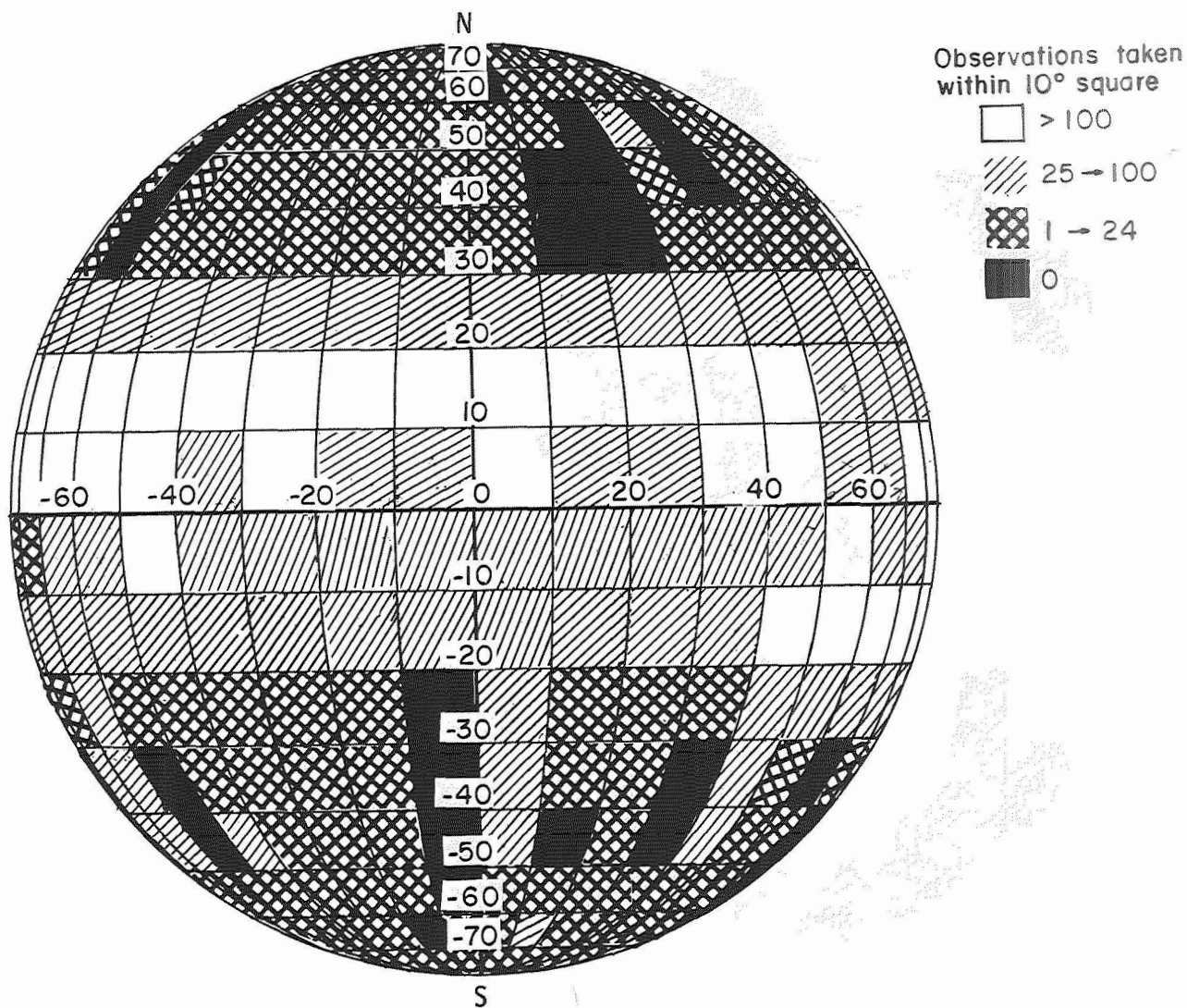
Degree and order	9	11	13	13	13
Number of observations	9126	9088	9088	12 600	20 148
GM	4902.806	4902.813	4902.807	4902.861	4902.844 ± 0.032
C ₂₀	-2.043 × 10 ⁻⁴	-2.298 × 10 ⁻⁴	-2.173 × 10 ⁻⁴	-2.071 × 10 ⁻⁴	-2.038 ± 0.147 × 10 ⁻⁴
C ₂₂	2.197 × 10 ⁻⁵	2.338 × 10 ⁻⁵	2.212 × 10 ⁻⁵	2.242 × 10 ⁻⁵	2.485 ± 0.244 × 10 ⁻⁵
C ₃₁	2.218 × 10 ⁻⁵	2.059 × 10 ⁻⁵	2.513 × 10 ⁻⁵	2.437 × 10 ⁻⁵	2.415 ± 0.262 × 10 ⁻⁵

TABLE IV.- ESTIMATES OF LUNAR MOMENTS OF INERTIA

Selenographic inertia tensor/Ma ²			Principal moments of inertia/Ma ²	
	X	Y	Z	
X	0.402093	0.000000	0.000011	0.402092 ± 0.02
Y	.000000	.402192	.000013	.402191 ± 0.02
Z	.000011	.000013	.402346	.402348 ± 0.02

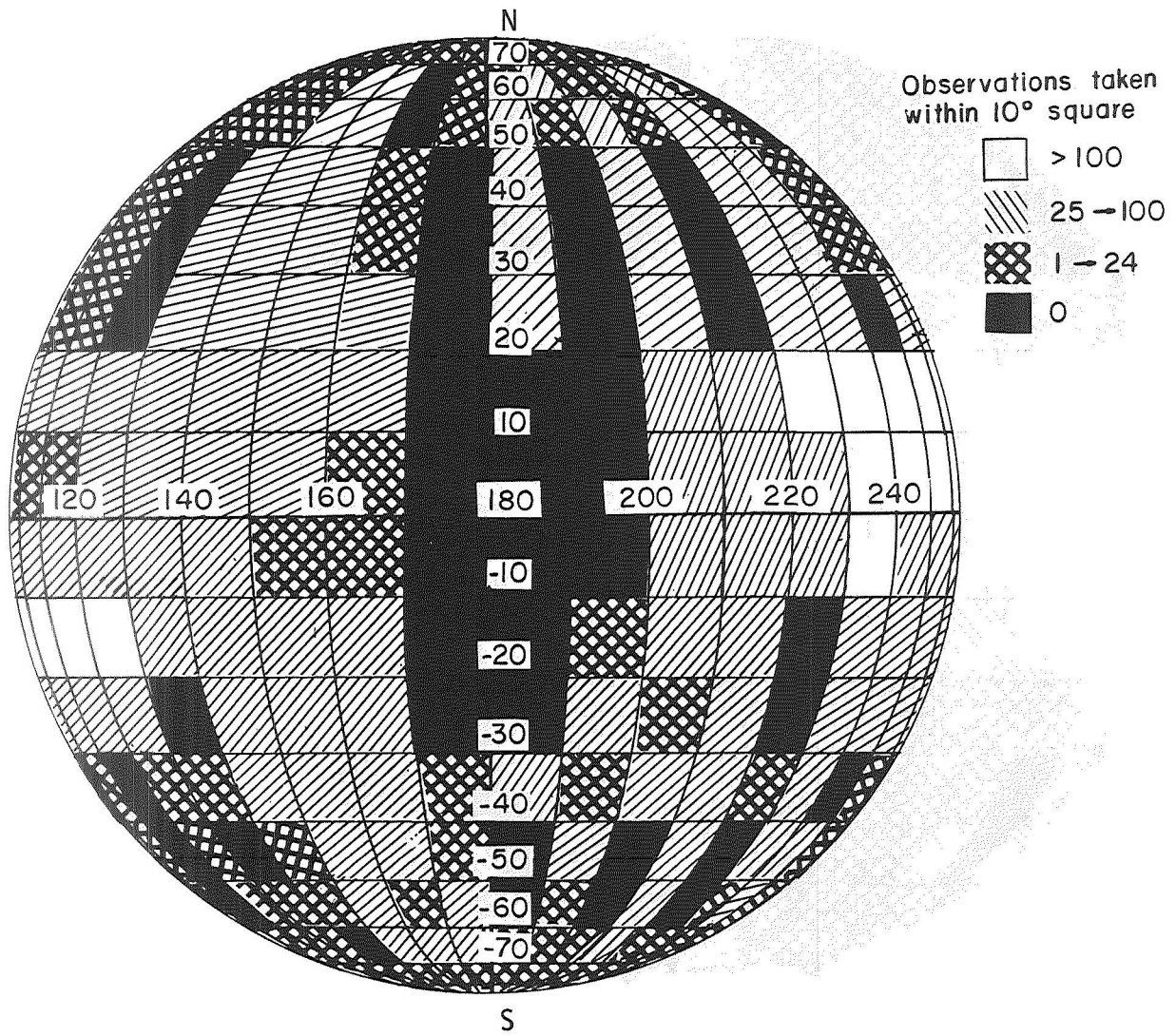
TABLE V.- POINT SOURCE APPROXIMATIONS

Site	Mass/Lunar mass	Radius, km	Latitude, deg	Longitude, deg
Imbrium	7.68 × 10 ⁻⁵	1450	33.8	16.3
Serenitatis	4.17 × 10 ⁻⁵	1546	29.0	-20.5



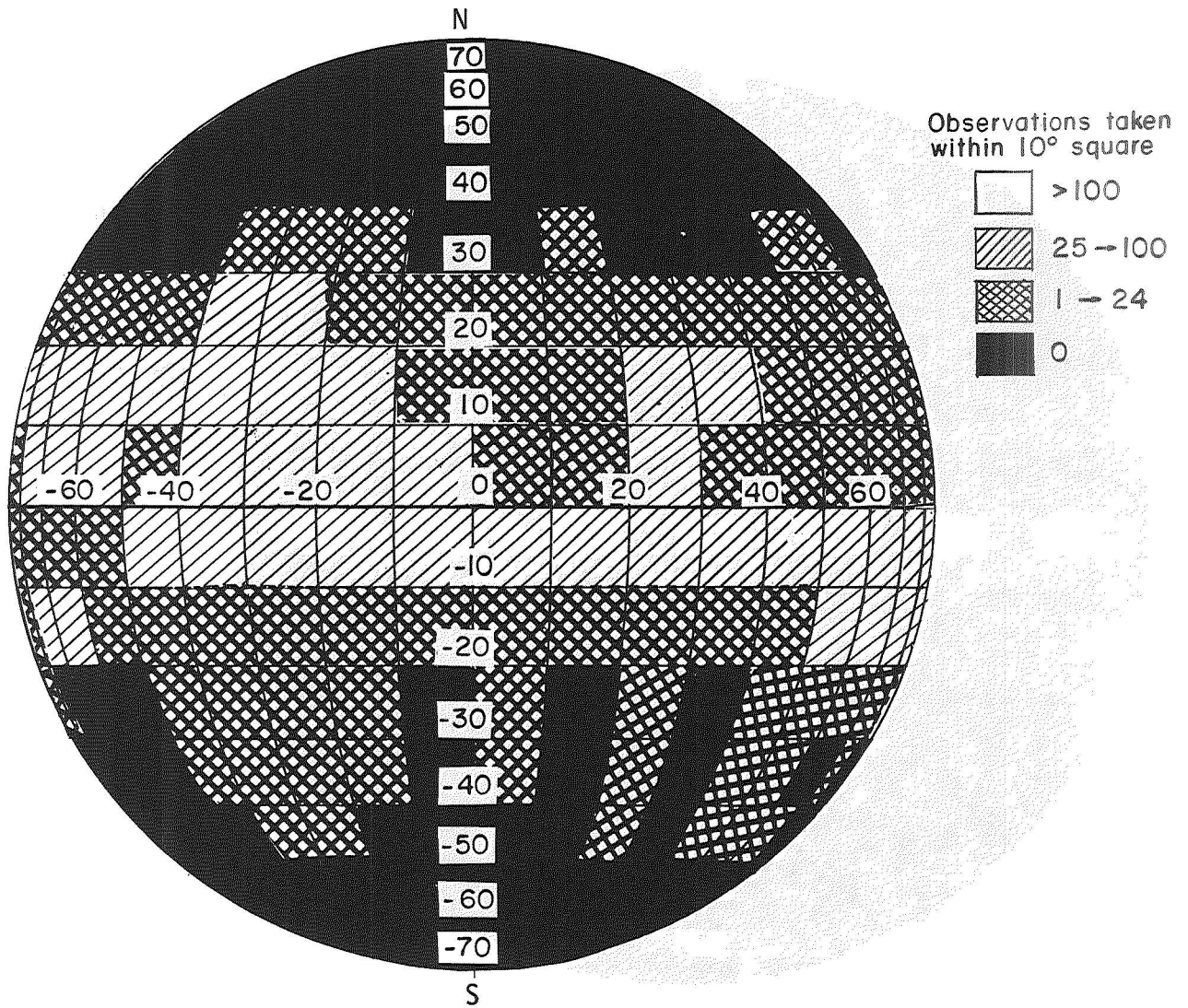
(a) Lunar near side.

Figure 1.- Total data coverage.



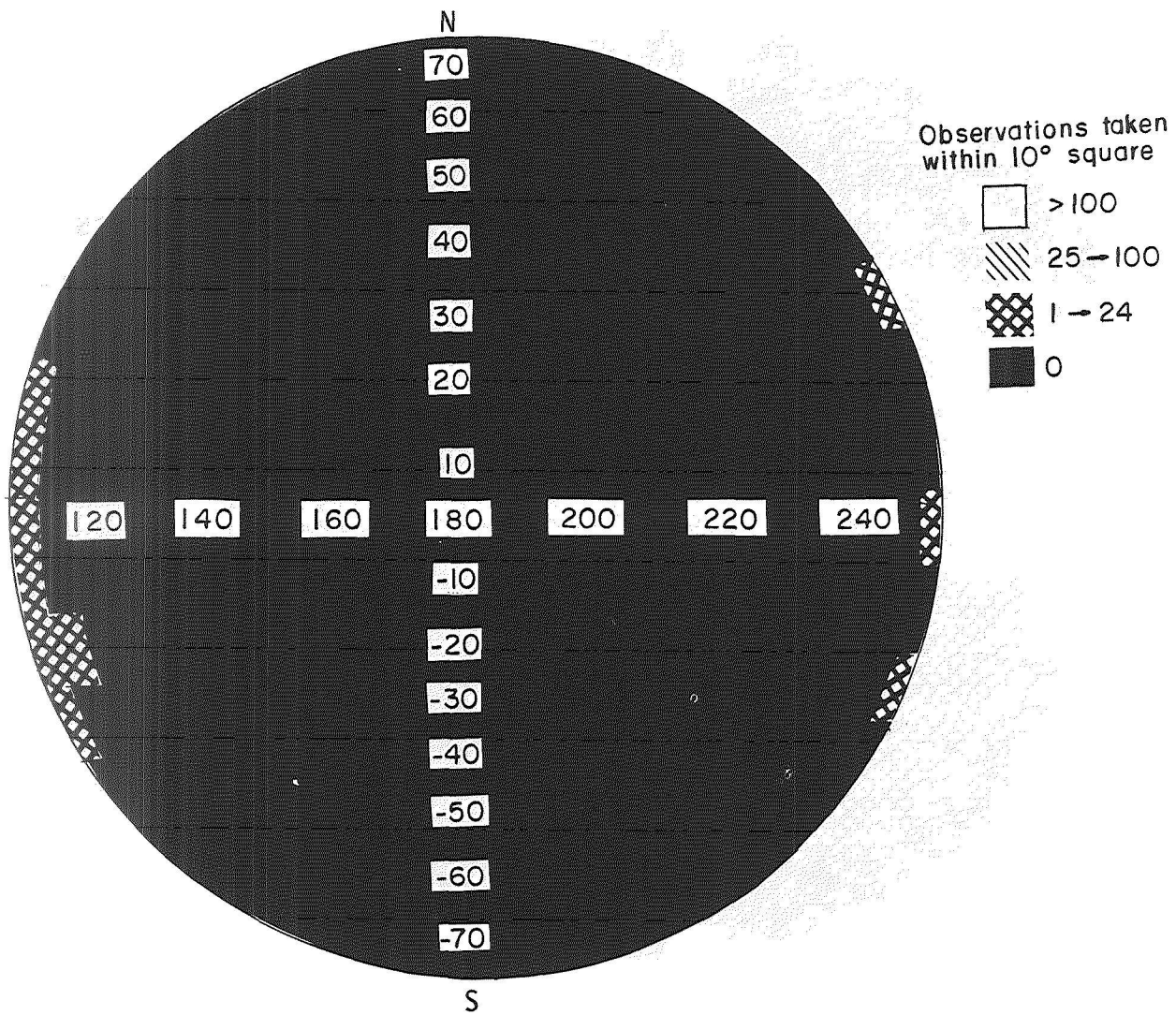
(b) Lunar far side.

Figure 1.- Concluded.



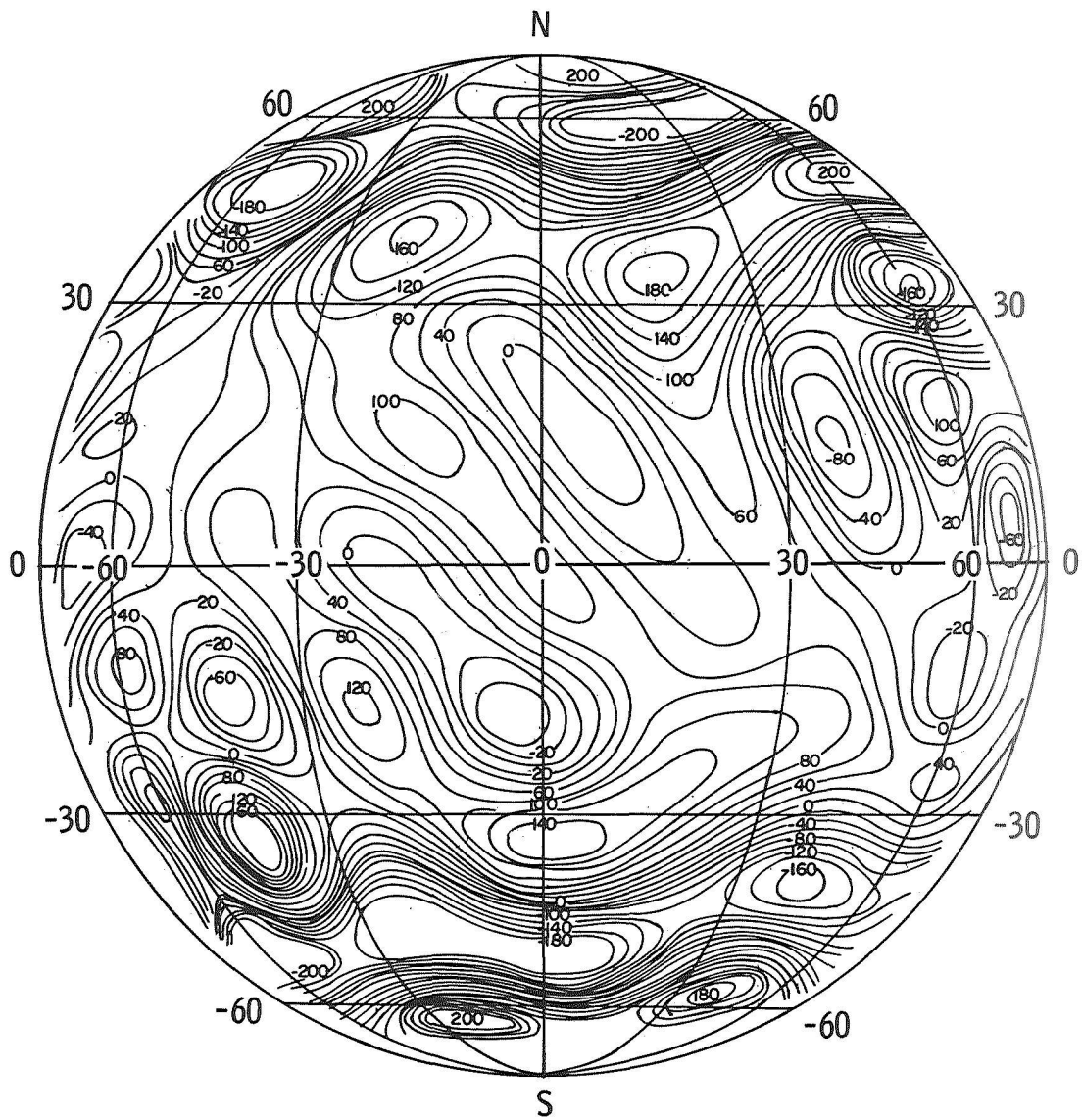
(a) Lunar near side.

Figure 2.- Observations taken when the spacecraft was below 200 km altitude.



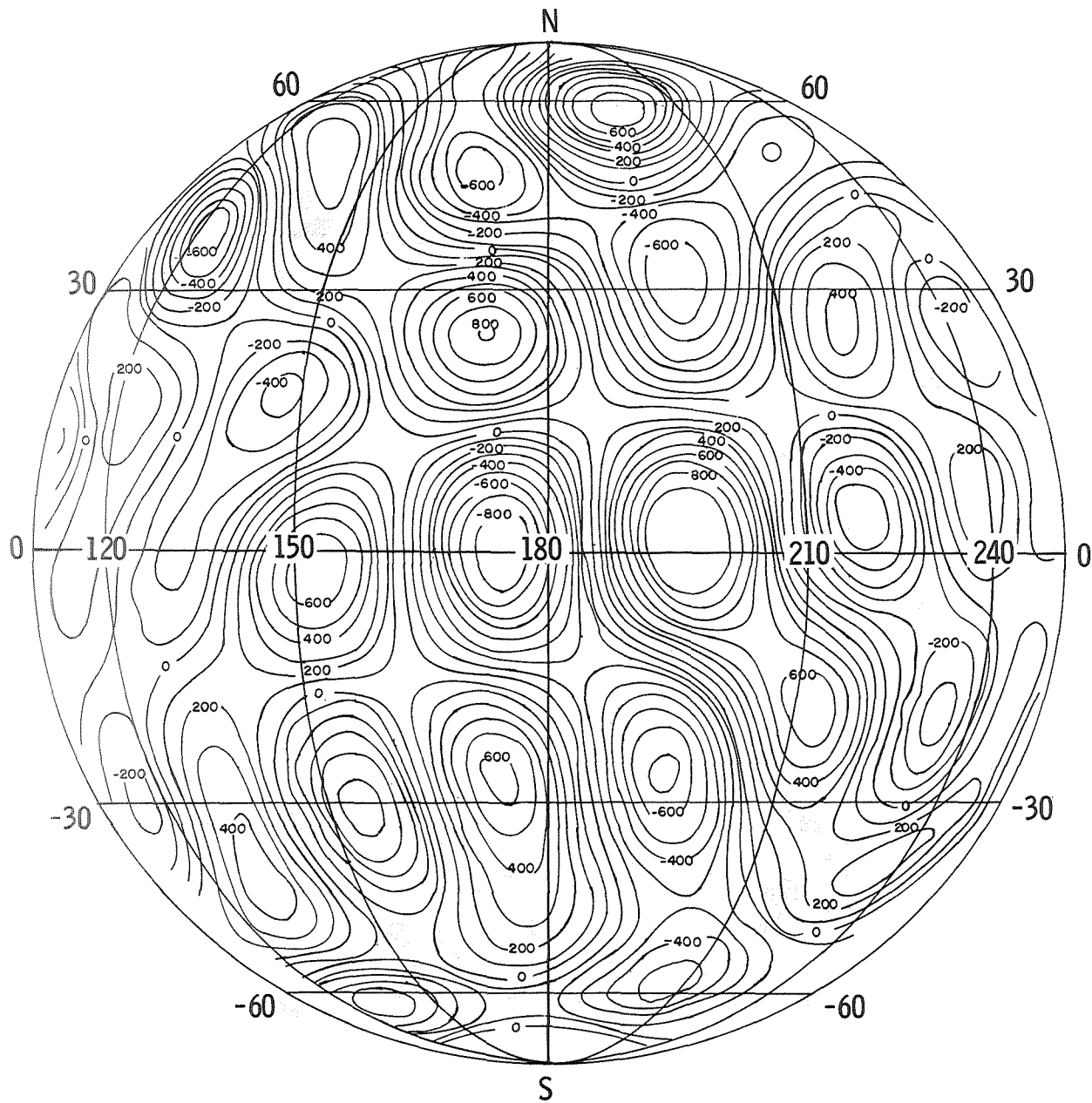
(b) Lunar far side.

Figure 2.- Concluded.



(a) Lunar near side.

Figure 3.- Estimate of variations in gravitational acceleration (milligals).



(b) Lunar far side.

Figure 3.- Concluded.

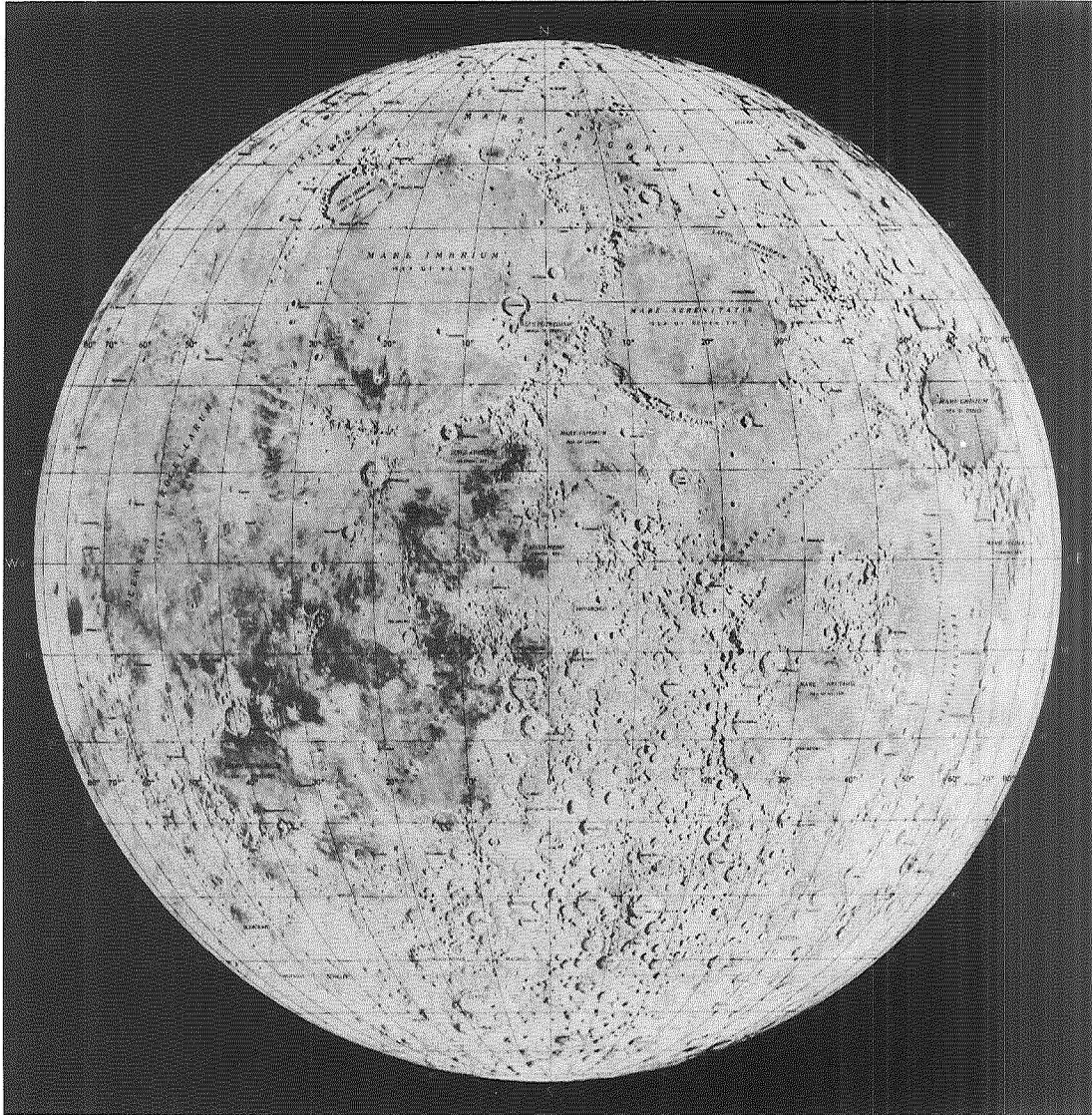


Figure 4.- Map of lunar near side.

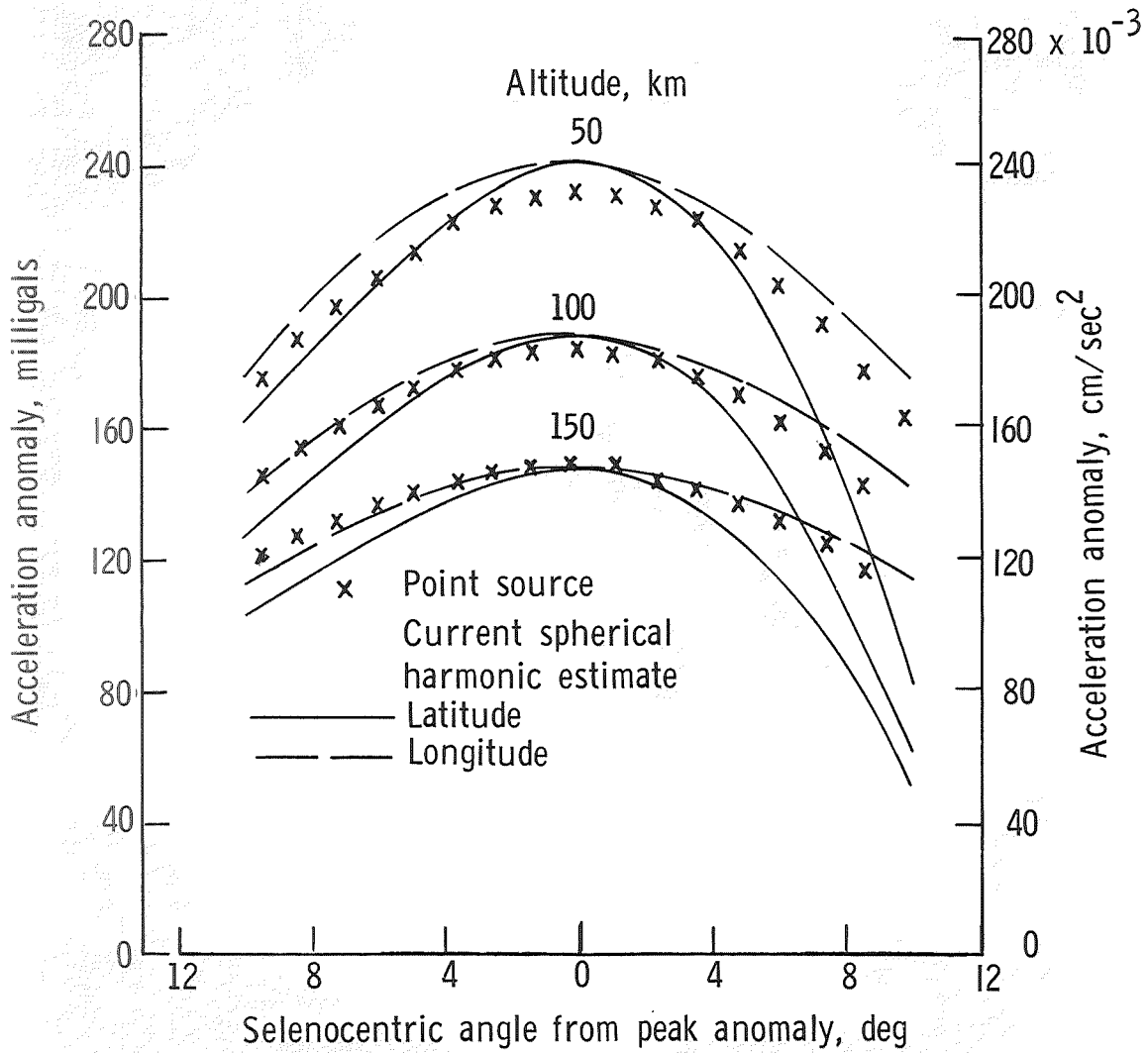


Figure 5.- Point source and spherical harmonic estimates of the Serenitatis gravitational anomaly as function of latitude and longitude. 1 milligal = $1 \times 10^{-3} \text{ cm}/\text{sec}^2$.

NATIONAL AERONAUTICS AND SPACE ADMINISTRATION
WASHINGTON, D. C. 20546

OFFICIAL BUSINESS
PENALTY FOR PRIVATE USE \$300

FIRST CLASS MAIL



POSTAGE AND FEES PAID
NATIONAL AERONAUTICS AND
SPACE ADMINISTRATION

POSTMASTER: If Undeliverable (Section 153,
Postal Manual) Do Not Return

"The aeronautical and space activities of the United States shall be conducted so as to contribute . . . to the expansion of human knowledge of phenomena in the atmosphere and space. The Administration shall provide for the widest practicable and appropriate dissemination of information concerning its activities and the results thereof."

— NATIONAL AERONAUTICS AND SPACE ACT OF 1958

NASA SCIENTIFIC AND TECHNICAL PUBLICATIONS

TECHNICAL REPORTS: Scientific and technical information considered important, complete, and a lasting contribution to existing knowledge.

TECHNICAL NOTES: Information less broad in scope but nevertheless of importance as a contribution to existing knowledge.

TECHNICAL MEMORANDUMS: Information receiving limited distribution because of preliminary data, security classification, or other reasons.

CONTRACTOR REPORTS: Scientific and technical information generated under a NASA contract or grant and considered an important contribution to existing knowledge.

TECHNICAL TRANSLATIONS: Information published in a foreign language considered to merit NASA distribution in English.

SPECIAL PUBLICATIONS: Information derived from or of value to NASA activities. Publications include conference proceedings, monographs, data compilations, handbooks, sourcebooks, and special bibliographies.

TECHNOLOGY UTILIZATION PUBLICATIONS: Information on technology used by NASA that may be of particular interest in commercial and other non-aerospace applications. Publications include Tech Briefs, Technology Utilization Reports and Technology Surveys.

Details on the availability of these publications may be obtained from:

SCIENTIFIC AND TECHNICAL INFORMATION OFFICE
NATIONAL AERONAUTICS AND SPACE ADMINISTRATION
Washington, D.C. 20546